NATIONAL UNIVERSITY OF HO CHI MINH CITY
UNIVERSITY OF SCIENCE

UNDERGRADUATE THESIS

Three-band tight binding model for TMD monolayers in the presence of a magnetic field

Ho Chi Minh City, 2025

Sutdent: Tran Khoi Nguyen
Supervisor: Dr. Huynh Thanh Duc

TABLE OF CONTENTS

LIST OF FIGURES

CHƯƠNG 1

INTRODUCTION

CHƯƠNG 2

METHOD

2.1 Three-band tight binding method without magnetic field

The time-indepentdent Schrödinger equation for an eletron in the crystal has the form

$$\left[-\frac{\hbar^2\nabla^2}{2m}+U_0(\mathbf{r})\right]=\psi_{\lambda,\mathbf{k}}(\mathbf{r})=\varepsilon_\lambda(\mathbf{k})\psi_{\lambda,\mathbf{k}}(\mathbf{r}), \tag{2.1}$$

where $U_0(\mathbf{r})$ is the periodic lattice potential, $\psi_{\lambda,\mathbf{k}}(\mathbf{r})$ is the Bloch wavefunction of an electron in band λ with wave vector $\mathbf{k}$ and $\varepsilon_\lambda(\mathbf{k})$ is the band structure.

In the tight binding model(TBM), the single-electron Bloch wavefunction can be expressed in terms of atomic orbitals as follows

$$\psi_{\lambda,\mathbf{k}}(\mathbf{r})=\sum_{j,i}C_{ji}^{\lambda}(\mathbf{k})\sum_{\mathbf{R}}e^{i\mathbf{k}\cdot(\mathbf{R}+\mathbf{r_i})}\phi_j(\mathbf{r}-\mathbf{R}-\mathbf{r}_i), \tag{2.2}$$

where $\phi_j(\mathbf{r}-\mathbf{R}-\mathbf{r}_i)$ is the orbital j of an atom i localized on a lattice site $\mathbf{R}$, in which $\mathbf{r}_i$ is the relavetive position of the atom i in the unit cell, and $C_{ji}^{\lambda}(\mathbf{k})$ are the coefficents of linear expansion.

The unit cell of transition dichalcogenide(TMDC) monolayers involve one transition metal atom M and two chalcogenide atoms X. From the previous first principle calculations, it is shown that the electron states near the band edges of MX_2 are mainly contributed from the three d orbital of M atom, namely $d_{z^2}, d_{xy}, d_{x^2-y^2}$ [1]. This model is called the three-band tight binding model. The three orbitals's wave function of M

atom are denoted as

$$|\phi_1\rangle = |d_{z^2}\rangle\,; \quad |\phi_2\rangle = \left|d_{xy}\right\rangle\,; \quad |\phi_3\rangle = \left|d_{x^2-y^2}\right\rangle\,. \tag{2.3}$$

The Bloch wavefunction in this model has the form

$$\psi_{\lambda,\mathbf{k}}(\mathbf{r}) = \sum_{j=1}^{3} C_j^{\lambda}(\mathbf{k}) \sum_{\mathbf{R}} e^{i\mathbf{k}\cdot\mathbf{R}} \phi_j(\mathbf{r}-\mathbf{R}). \tag{2.4}$$

The coefficents $C_j^{\lambda}(\mathbf{k})$ are the solutions of the eigenvalue equation

$$\sum_{jj'}^{3} \left[H_{jj'}(\mathbf{k}) - \varepsilon_{\lambda}(\mathbf{k}) S_{jj'}(\mathbf{k})\right] C_j^{\lambda}(\mathbf{k}) = 0, \tag{2.5}$$

where

$$H_{jj'}(\mathbf{k}) = \sum_{\mathbf{R}} e^{i\mathbf{k}\cdot\mathbf{R}} \left\langle \phi_j(\mathbf{r})\right| \left[-\frac{\hbar^2\nabla^2}{2m} + U_0(\mathbf{r})\right] \left|\phi_{j'}(\mathbf{r}-\mathbf{R})\right\rangle\,, \tag{2.6}$$

and

$$S_{jj'}(\mathbf{k}) = \sum_{\mathbf{R}} \left\langle \phi_j(\mathbf{r})\middle|\phi_{j'}(\mathbf{r}-\mathbf{R})\right\rangle \approx \delta_{jj'}. \tag{2.7}$$

Three-band tight binding model takes into account the nearest neighbor hopping is called the three-band nearest-neighbor(NN) model. This model agrees well with the ab initio calculation for the band structure near the band edges, but the significantly deviate from the latter in other regions. This is because the three-band approximation neglects the p orbitals of X atoms which still have substanial contributions to the conduction bands at Γ and valence bands at M. The matrix elements of the TB Hamiltonian(pt) are

$$H_{\mu\mu} \tag{2.8}$$

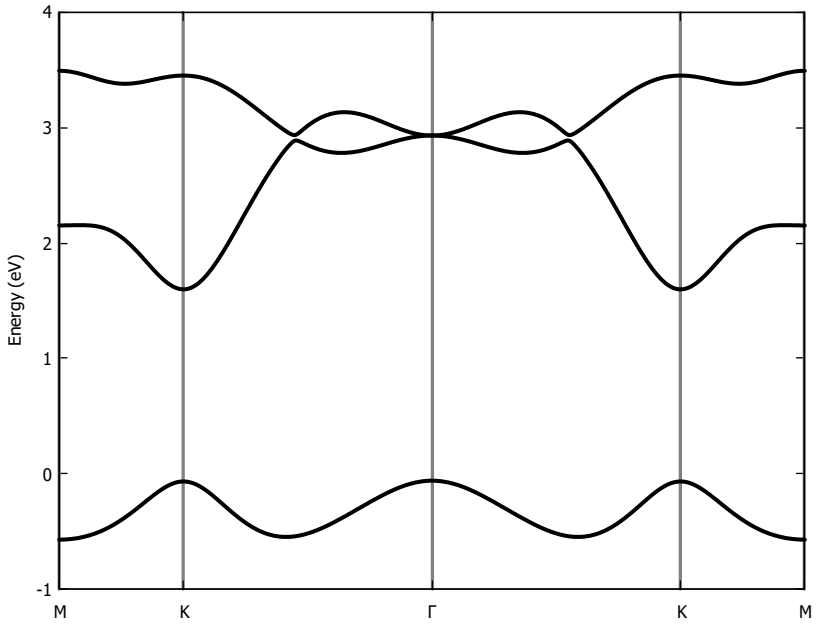

Hình 2.1

2.2 Three-band tight binding method under a magnetic field

Under a uniform magnetic field given by a vector potential $\mathbf{A}(\mathbf{r})$ the single electron Hamiltonian changes into

$$H = \frac{\left(-i\hbar\boldsymbol{\nabla} + e\mathbf{A}(\mathbf{r})\right)^2}{2m} + U_0(\mathbf{r}) + g^*\mu_B\mathbf{B}\cdot\mathbf{L}, \tag{2.9}$$

where $\mu_B = \dfrac{e\hbar}{2m}$ is Bohr magneton, g^* is an effective Landé g-factor, $\mathbf{B} = \boldsymbol{\nabla}\times\mathbf{A}$ is the uniform magnetic field, and $\mathbf{L}$ is the angular momentum. It is possible to add a phase factor to the tight binding wavefunction

$$\psi_{\lambda,\mathbf{k}}(\mathbf{r}) = \sum_{j=1}^{3} C_j^{\lambda} \sum_{\mathbf{R}} e^{i\mathbf{k}\cdot\mathbf{R}} e^{i\theta_{\mathbf{R}(\mathbf{r})}} \phi_j(\mathbf{r}-\mathbf{R}). \tag{2.10}$$

We now have

$$H_{jj'}(\mathbf{k}) = H'_{jj'}(\mathbf{k}) + H^Z_{jj'}(\mathbf{k}), \tag{2.11}$$

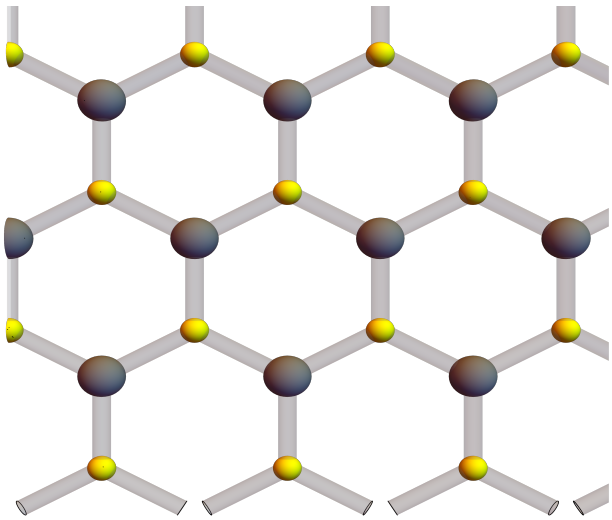

Hình 2.2: Top view of monolayer MX_2. The large sphere is M atom and the small sphere is X.

where

$$\begin{aligned} H_{jj'}(\mathbf{k}) &= \sum_{\mathbf{R}} e^{i\mathbf{k}\cdot\mathbf{R}} \left\langle \phi_j(\mathbf{r}) \right| e^{-i\theta_{\mathbf{0}}(\mathbf{r})} \left[\frac{(-i\hbar\boldsymbol{\nabla} + e\mathbf{A}(\mathbf{r}))^2}{2m} + U_0(\mathbf{r}) \right] e^{i\theta_{\mathbf{R}}(\mathbf{r})} \left| \phi_{j'}(\mathbf{r}-\mathbf{R}) \right\rangle \\ &= \sum_{\mathbf{R}} e^{i\mathbf{k}\cdot\mathbf{R}} \left\langle \phi_j(\mathbf{r}) \right| e^{i(\theta_{\mathbf{R}}-\theta_{\mathbf{0}})} \left[\frac{(-i\hbar\boldsymbol{\nabla} + e\mathbf{A} + \hbar\boldsymbol{\nabla}\theta_{\mathbf{R}})^2}{2m} + U_0(\mathbf{r}) \right] \left| \phi_{j'}(\mathbf{r}-\mathbf{R}) \right\rangle , \end{aligned} \tag{2.12}$$

and

$$H^Z_{jj'}(\mathbf{k}) = g^*\mu_B \mathbf{B} \cdot \sum_{\mathbf{R}} \left\langle \phi_j(\mathbf{r}) \right| e^{i(\theta_{\mathbf{R}}-\theta_{\mathbf{0}})} \mathbf{L} \left| \phi_{j'}(\mathbf{r}-\mathbf{R}) \right\rangle . \tag{2.13}$$

By choosing $\theta_{\mathbf{R}} = -\frac{e}{\hbar}\int_{\mathbf{R}}^{\mathbf{r}} \mathbf{A}(\mathbf{r}')\cdot d\mathbf{r}'$ as Peierls substitution, the Hamiltonian in Eq. (4) now reads

$$\begin{aligned} H_{jj'}(\mathbf{k}) &= \sum_{\mathbf{R}} e^{i\mathbf{k}\cdot\mathbf{R}} \left\langle \phi_j(\mathbf{r}) \right| e^{-\frac{ie}{\hbar}\int_{\mathbf{R}}^{\mathbf{r}} \mathbf{A}(\mathbf{r}')\cdot d\mathbf{r}' + \frac{ie}{\hbar}\int_{\mathbf{0}}^{\mathbf{r}} \mathbf{A}(\mathbf{r}')\cdot d\mathbf{r}'} \left[-\frac{\hbar^2\boldsymbol{\nabla}^2}{2m} + U_0(\mathbf{r}) \right] \left| \phi_{j'}(\mathbf{r}-\mathbf{R}) \right\rangle \\ &= \sum_{\mathbf{R}} e^{i\mathbf{k}\cdot\mathbf{R}} e^{\frac{ie}{\hbar}\int_{\mathbf{0}}^{\mathbf{R}} \mathbf{A}(\mathbf{r}')\cdot d\mathbf{r}'} \left\langle \phi_j(\mathbf{r}) \right| e^{-\frac{ie}{\hbar}\Phi_{\mathbf{R},\mathbf{r},\mathbf{0}}} \left[-\frac{\hbar^2\boldsymbol{\nabla}^2}{2m} + U_0(\mathbf{r}) \right] \left| \phi_{j'}(\mathbf{r}-\mathbf{R}) \right\rangle , \end{aligned} \tag{2.14}$$

where $\Phi_{\mathbf{R},\mathbf{r},\mathbf{0}} = \oint_{\mathbf{R},\mathbf{r},\mathbf{0}} \mathbf{A}(\mathbf{r}') \cdot d\mathbf{r}'$ is the closed loop line intergral of $\mathbf{A}$ along the triangle points $\mathbf{R}, \mathbf{r}, \mathbf{0}$, and $\int_{\mathbf{0}}^{\mathbf{R}} \mathbf{A}(\mathbf{r}') \cdot d\mathbf{r}'$ is the path intergral along the two points $\mathbf{R}, \mathbf{0}$. Besides that, we have used the fact that

$$\int_{\mathbf{R}}^{\mathbf{r}} \mathbf{A}(\mathbf{r}') \cdot d\mathbf{r}' + \int_{\mathbf{r}}^{\mathbf{0}} \mathbf{A}(\mathbf{r}') \cdot \mathbf{r}' = \Phi_{\mathbf{R},\mathbf{r},\mathbf{0}} - \int_{\mathbf{0}}^{\mathbf{R}} \mathbf{A}(\mathbf{r}') \cdot d\mathbf{r}'. \tag{2.15}$$

We can show that the flux term $\Phi_{\mathbf{R},\mathbf{r},\mathbf{0}}$ is negligibly small[2] by two observations. When $\mathbf{r}$ is far away from the lattice points $\mathbf{R}$ and $\mathbf{0}$, the flux is large but since the atomic orbitals are highly localized at these two lattice points, the value of the hopping term is very small and the whole hopping term goes to zero. While $\mathbf{r}$ is at or near any of these lattice points, the triangle formed is small, and assuming small magnetic field, the flux term $\Phi_{\mathbf{R},\mathbf{r},\mathbf{0}}$ goes to zero, which giving us the Hamiltonian as

$$H_{jj'}(\mathbf{k}) = \sum_{\mathbf{R}} e^{i\mathbf{k}\cdot\mathbf{R}} e^{\frac{ie}{\hbar}\int_{\mathbf{0}}^{\mathbf{R}} \mathbf{A}(\mathbf{r}')\cdot d\mathbf{r}'} \left\langle \phi_j(\mathbf{r}) \right| \left[-\frac{\hbar^2 \boldsymbol{\nabla}^2}{2m} + U_0(\mathbf{r}) \right] \left| \phi_{j'}(\mathbf{r} - \mathbf{R}) \right\rangle, \tag{2.16}$$

$$H^Z_{jj'}(\mathbf{k}) = g^* \mu_B \mathbf{B} \cdot \sum_{\mathbf{R}} e^{i\mathbf{k}\cdot\mathbf{R}} e^{\frac{ie}{\hbar}\int_{\mathbf{0}}^{\mathbf{R}} \mathbf{A}(\mathbf{r}')\cdot d\mathbf{r}'} \left\langle \phi_j(\mathbf{r}) \right| \mathbf{L} \left| \phi_{j'}(\mathbf{r} - \mathbf{R}) \right\rangle. \tag{2.17}$$

Considering only nearest neighbor(NN) hopping, Eq (2.9) becomes

$$\begin{aligned}
H_{jj'}(\mathbf{k}) &= \sum_{\mathbf{R}} e^{\frac{ie}{\hbar}\int_0^{\mathbf{R}} A(\mathbf{r}')d\mathbf{r}'} e^{i\mathbf{k}\cdot\mathbf{R}} E_{jj'}(\mathbf{R}) \\
&= E_{jj'}(\mathbf{0}) + e^{\frac{ie}{\hbar}\int_0^{\mathbf{R_1}} \mathbf{A}(\mathbf{r}')\cdot d\mathbf{r}'} e^{i\mathbf{k}\cdot\mathbf{R_1}} E_{jj'}(\mathbf{R_1}) \\
&+ e^{\frac{ie}{\hbar}\int_0^{\mathbf{R_2}} \mathbf{A}(\mathbf{r}')\cdot d\mathbf{r}'} e^{i\mathbf{k}\cdot\mathbf{R_2}} E_{jj'}(\mathbf{R_2}) + e^{\frac{ie}{\hbar}\int_0^{\mathbf{R_3}} \mathbf{A}(\mathbf{r}')\cdot d\mathbf{r}'} e^{i\mathbf{k}\cdot\mathbf{R_3}} E_{jj'}(\mathbf{R_3}) \\
&+ e^{\frac{ie}{\hbar}\int_0^{\mathbf{R_4}} \mathbf{A}(\mathbf{r}')\cdot d\mathbf{r}'} e^{i\mathbf{k}\cdot\mathbf{R_4}} E_{jj'}(\mathbf{R_4}) + e^{\frac{ie}{\hbar}\int_0^{\mathbf{R_5}} \mathbf{A}(\mathbf{r}')\cdot d\mathbf{r}'} e^{i\mathbf{k}\cdot\mathbf{R_5}} E_{jj'}(\mathbf{R_5}) \\
&+ e^{\frac{ie}{\hbar}\int_0^{\mathbf{R_6}} \mathbf{A}(\mathbf{r}')\cdot d\mathbf{r}'} e^{i\mathbf{k}\cdot\mathbf{R_6}} E_{jj'}(\mathbf{R_6}).
\end{aligned} \tag{2.18}$$

In the presence of a perpendicular magnetic field $\mathbf{B}\hat{z}$ with the vector potential $\vec{A} = (0, Bx, 0)$. For convenience, let us switch to a shorthand notation for these extra terms and define

$$\theta^{m',n'}_{m,n} \equiv -\frac{e}{\hbar} \int_{m,n}^{m',n'} \vec{A} \cdot d\mathbf{r}. \tag{2.19}$$

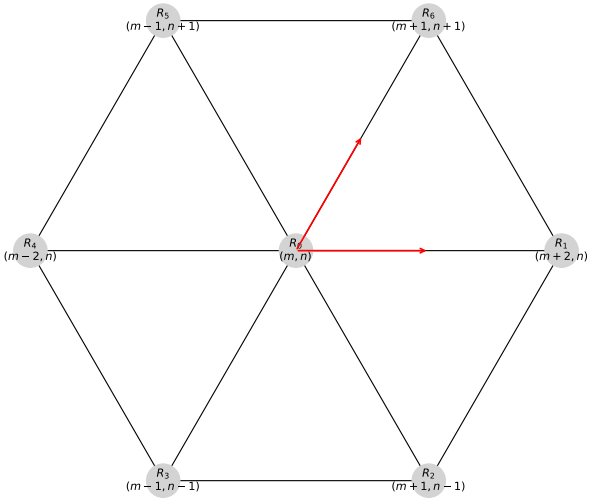

Hình 2.3: Site index

With the given Landau gauge, the line intergral $\int \vec{A} \cdot d\mathbf{r}$ is evaluated to $\int Bxdy$. Let us now express the Hamiltonian from the zero-field are given by[1] with the transform hopping parameters, noting that the NN coordinates are $x = \frac{ma}{2}(m = \pm 1, \pm 2)$ and $y = \frac{na\sqrt{3}}{2}(n = 0, \pm 1)$, a being the lattice constant, are shown in Fig (2.2). Since $dy = 0$ along the x direction, $\theta_{m,n}^{m\pm 2,n} = 0$, and using *ansatz* $x = \frac{ma}{2}$ for lattice site, the $\theta_{m,n}^{m',n'}$ can be written as

$$\theta_{m,n}^{m',n'} = \begin{cases} 0 & m' = m \pm 2, n' = n, \\ \pm\frac{e}{\hbar}\frac{Ba^2\sqrt{3}}{4}(m + 1/2) & m' = m + 1, n' = n \pm 1, \\ \pm\frac{e}{\hbar}\frac{Ba^2\sqrt{3}}{4}(m - 1/2) & m' = m - 1, n' = n \pm 1. \end{cases} \tag{2.20}$$

Identifying $\frac{Ba^2\sqrt{3}}{4}$ as the magnetic flux Φ passing through per unit cell and h/e as the flux quantum Φ_0, then we have

$$\begin{aligned} H_{jj'}(\mathbf{k}) = E_{jj'}(\mathbf{0}) &+ e^{i\theta_{m,n}^{m',n'}} e^{i\mathbf{k}\cdot\mathbf{R}_1} E_{jj'}(\mathbf{R}_1) + e^{i\theta_{m,n}^{m',n'}} e^{i\mathbf{k}\cdot\mathbf{R}_2} E_{jj'}(\mathbf{R}_2) \\ &+ e^{i\theta_{m,n}^{m',n'}} e^{i\mathbf{k}\cdot\mathbf{R}_3} E_{jj'}(\mathbf{R}_3) + e^{i\theta_{m,n}^{m',n'}} e^{i\mathbf{k}\cdot\mathbf{R}_4} E_{jj'}(\mathbf{R}_4) \\ &+ e^{i\theta_{m,n}^{m',n'}} e^{i\mathbf{k}\cdot\mathbf{R}_5} E_{jj'}(\mathbf{R}_5) + e^{i\theta_{m,n}^{m',n'}} e^{i\mathbf{k}\cdot\mathbf{R}_6} E_{jj'}(\mathbf{R}_6). \end{aligned} \tag{2.21}$$

The Hamiltonian depends on the site index m and does not invariant under the translation of a lattice vector along the x axis. In order to restore this invariance, we can look at the case where the ratio of magnetic flux and flux quanta is a rational number $\Phi/\Phi_0 = p/q$. This mean, we have expand the unit cell in the x direction, the Hamilto-

nian becomes invariant under translational, allowing us to define what we will call the magnetic unit cell, which is consisting of q M-atoms. We define a new basis set of $3q$ atomic orbitals $\phi^j_\mu(x,y) = \phi^j_\mu(ma/2, y)$ where $m = 1, 2, ...q$. Note that

$$\begin{cases} e^{ik_x a}\phi_j\left(m\frac{a}{2}, y\right) = \phi_j\left((m+2)\frac{a}{2}, y\right), \\ e^{-ik_x a}\phi_j\left(m\frac{a}{2}, y\right) = \phi_j\left((m-2)\frac{a}{2}, y\right), \\ e^{\pm ik_x\frac{a}{2}}e^{\pm ik_y\frac{a\sqrt{3}}{2}}\phi_j\left(m\frac{a}{2}, n\frac{a\sqrt{3}}{2}\right) = \phi_j\left((m\pm 1)\frac{a}{2}, (n\pm 1)\frac{a\sqrt{3}}{2}\right). \end{cases} \tag{2.22}$$

Consequently the Hamiltonian matrix in the new basis is written as

$$\begin{aligned} H_{jj'}(\mathbf{k}) = {} & E_{jj'}(\mathbf{0})\delta_{m,m} + e^{i\theta^{m',n'}_{m,n}} E_{jj'}(\mathbf{R}_1)\delta_{m,m+2}\delta_{n,n} + e^{i\theta^{m',n'}_{m,n}} E_{jj'}(\mathbf{R}_2)\delta_{m,m+1}\delta_{n,n-1} \\ & + e^{i\theta^{m',n'}_{m,n}} E_{jj'}(\mathbf{R}_3)\delta_{m,m-1}\delta_{n,n-1} + e^{i\theta^{m',n'}_{m,n}} E_{jj'}(\mathbf{R}_4)\delta_{m,m+2}\delta_{n,n} \\ & + e^{i\theta^{m',n'}_{m,n}} E_{jj'}(\mathbf{R}_5)\delta_{m,m-1}\delta_{n,n+1} + e^{i\theta^{m',n'}_{m,n}} E_{jj'}(\mathbf{R}_6)\delta_{m,m+1}\delta_{n,n+1}. \end{aligned} \tag{2.23}$$

By substituting Eq (2.15) and Eq (2.13) into Eq (2.16), we have

$$\begin{aligned} H_{jj'}(\mathbf{k}) = {} & E_{jj'}(\mathbf{0}) + E_{jj'}(\mathbf{R}_1) + e^{-2i\pi(m+1/2)p/q}e^{-i\beta}E_{jj'}(\mathbf{R}_2) \\ & + e^{-2i\pi(m-1/2)p/q}e^{-i\beta}E_{jj'}(\mathbf{R}_3) + E_{jj'}(\mathbf{R}_4) \\ & + e^{-2i\pi(m-1/2)p/q}e^{i\beta}E_{jj'}(\mathbf{R}_5) + e^{2i\pi(m+1/2)p/q}e^{i\beta}E_{jj'}(\mathbf{R}_6). \end{aligned} \tag{2.24}$$

Now, for given flux ratio p/q, only the q determines the periodicity of the magnetic cell assuming p and q are mutually prime numbers. When we plot the band energies while varying the p, we obtain the famous Hofstadter butterfly[3], a complex fractal structure as seen in Fig. 2.3. This structure is generated at the $K = (\frac{4\pi}{3a}, 0)$ k-point. This fractal spectrum is a result of two competing effects, lattice periodicity and magnectic unit cell periodicity enforced by the presence of the magnetic field. Eq. 2.16 give the following matrix which must be diagonalized to obtain the energy eigenvalues.

The magnetic field enters the TB Hamiltonian only through the fraction p/q, which is the magnetic flux through the primitive unit cell of the lattice. In general, as the lattice geometry evolves, the area of the primitive unit cell changes $(m + 1/2)$ times.

The spectrum has various symmetries: It is only show that the flux q is affects the spectrum, so if p/q changed to $p/q + c$ while c any interger, the spectrum is unchanged. The spectrum is also unchanged on changing p/q to $-p/q$, because if ψ is an eigenstate withe energy for field p/q, then its complex conjugate ψ^* is an engenstate with the same energy for field $-p/q$. These two symmetries are not special to the MX_2's case. The third symmetry is that if p/q is changed to $p/q + 1/2$, this is the same as changing t_i,

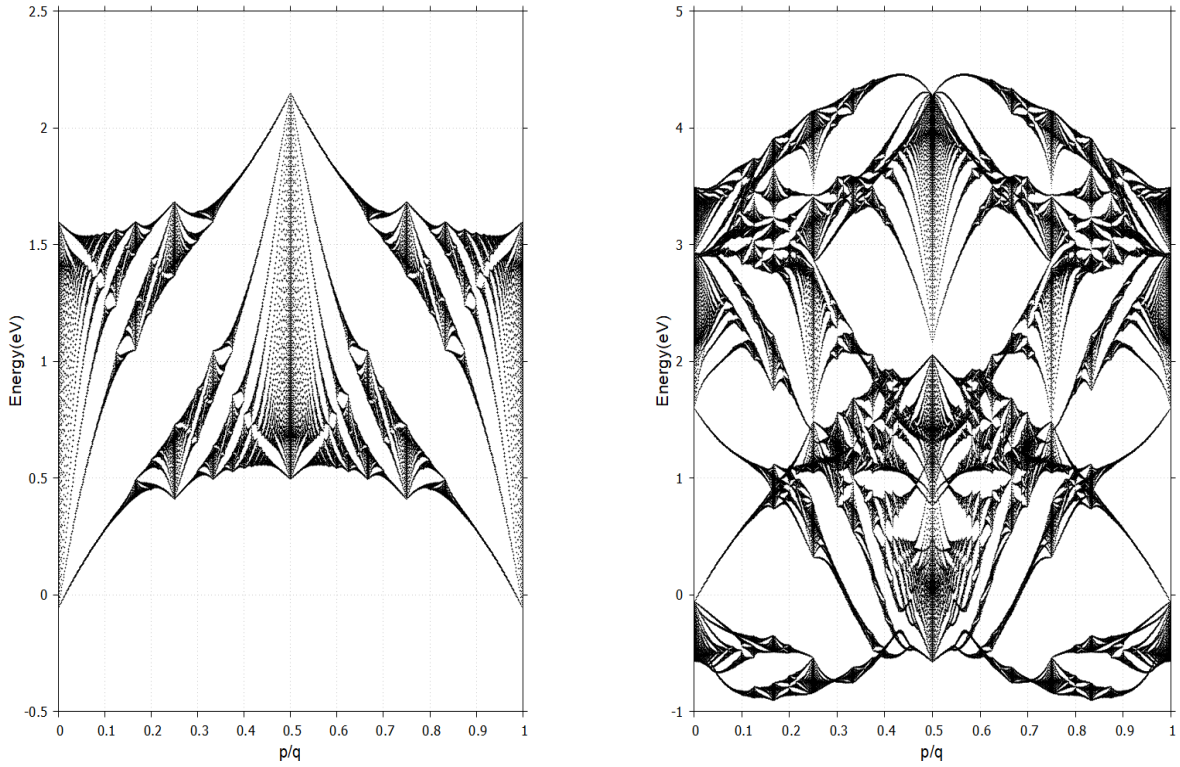

Hình 2.4: Hofstadter's butterfly for one band $|dz\rangle \equiv \left|\phi_1^1(x,y)\right\rangle$(left) and all band(right) with $q = 797$ and vary p from 1 to q with field strength $B_0 = 4.6928 \times 10^4$ T.

which are hopping energies, to $-t_i$, this leads to the inverting of the spectrum.

Using Eq (2.16), we obtain the eigenvalue equation $H\phi_\mu^j = E\phi_\mu^j$ and

$$H = \begin{pmatrix} h_0 & h_1 & h_2 \\ h_1^* & h_{11} & h_{12} \\ h_2^* & h_{12}^* & h_{22} \end{pmatrix} \tag{2.25}$$

where

$$h_0 = \begin{pmatrix} \epsilon_1 & 2t_0\cos\zeta_1 & t_0 & 0 & \cdots & 0 & t_0 & 2t_0\cos\gamma_1 \\ 2t_0\cos\gamma_2 & \epsilon_1 & 2t_0\cos\zeta_2 & t_0 & 0 & \cdots & 0 & t_0 \\ t_0 & 2t_0\cos\gamma_3 & \epsilon_1 & 2t_0\cos\zeta_3 & t_0 & 0 & \cdots & 0 \\ \vdots & \vdots & \vdots & \ddots & \vdots & \vdots & \vdots & \vdots \\ t_0 & 0 & \cdots & 0 & t_0 & 2t_0\cos\gamma_{q-1} & \epsilon_1 & 2t_0\cos\zeta_{q-1} \\ 2t_0\cos\zeta_q & t_0 & \cdots & 0 & 0 & t_0 & 2t_0\cos\gamma_q & \epsilon_1 \end{pmatrix} \tag{2.26}$$

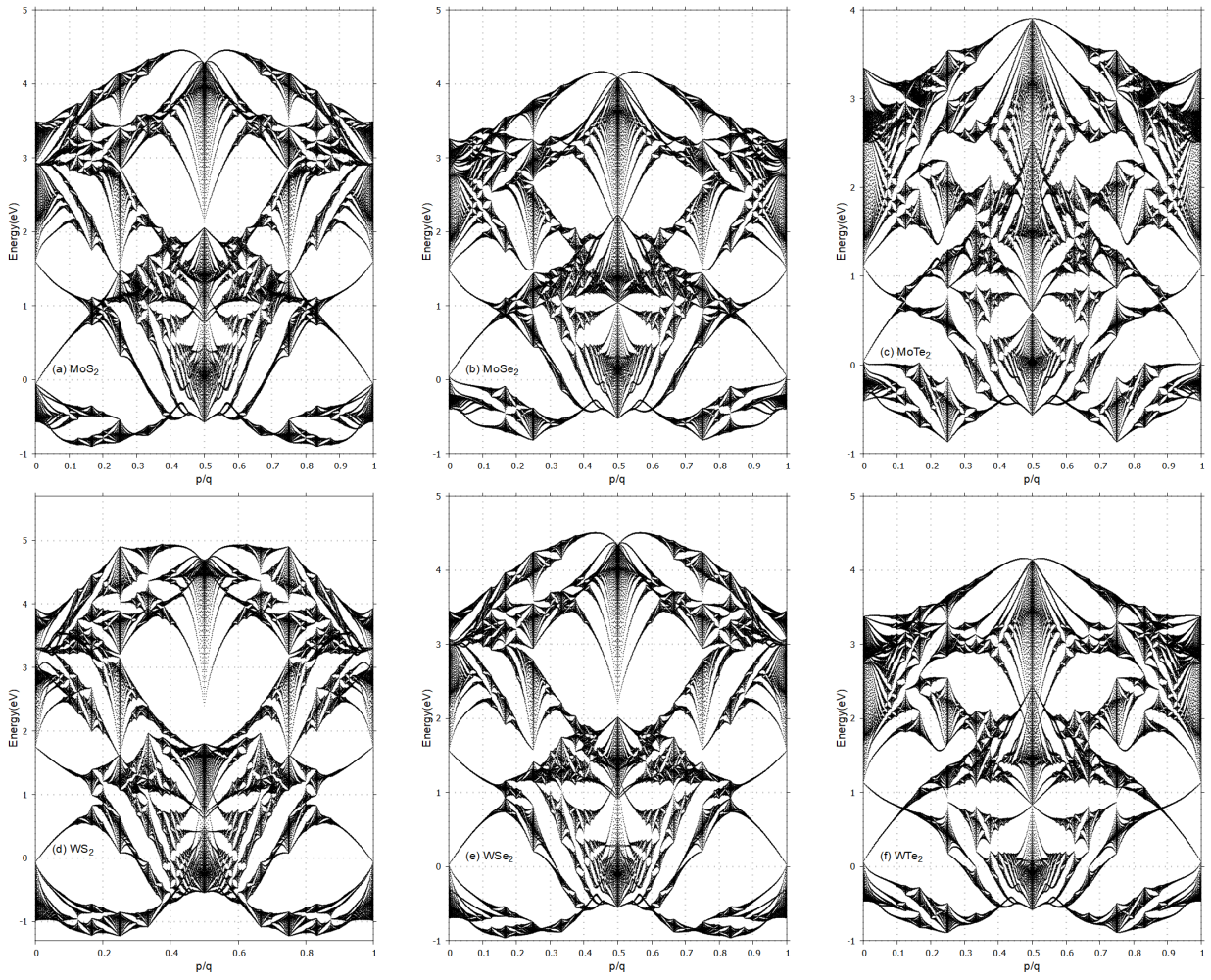

Hình 2.5: The Hofstadter's butterflies of MX_2 monolayers using GGA parameters from[1].

$$h_1 = \begin{pmatrix} 0 & 2t_1\cos\zeta_1 + i\sqrt{3}t_2\sin\zeta_1 & t_1 & 0 & \cdots & 0 & -t_1 & -2t_1\cos\gamma_1 - i\sqrt{3}t_2\sin\gamma_1 \\ -2t_1\cos\gamma_2 - i\sqrt{3}t_2\sin\gamma_2 & 0 & 2t_1\cos\zeta_2 + i\sqrt{3}t_2\sin\zeta_2 & t_1 & 0 & \cdots & 0 & -t_1 \\ -t_1 & -2t_1\cos\gamma_3 - i\sqrt{3}t_2\sin\gamma_3 & 0 & 2t_1\cos\zeta_3 + i\sqrt{3}t_2\sin\zeta_3 & t_1 & 0 & \cdots & 0 \\ \vdots & \vdots & \vdots & \vdots & \vdots & \vdots & \vdots & \vdots \\ t_1 & 0 & \cdots & 0 & -t_1 & -2t_1\cos\gamma_{q-1} - i\sqrt{3}t_2\sin\gamma_{q-1} & 0 & 2t_1\cos\zeta_{q-1} + i\sqrt{3}t_2\sin\zeta_{q-1} \\ 2t_1\cos\zeta_q + i\sqrt{3}t_2\sin\zeta_q & t_1 & \cdots & 0 & 0 & -t_1 & -2t_1\cos\gamma_q - i\sqrt{3}t_2\sin\gamma_q & 0 \end{pmatrix} \tag{2.27}$$

in which $\cos\zeta_m = \cos\left[\beta + 2\pi(m+1/2)p/q\right]$ and $\sin\gamma_m = \sin\left[\beta + 2\pi(m-1/2)p/q\right]$ and $h_0, h_1, h_2, h_{11}, h_{12}, h_{22}$ are sub-matrices have size $q \times q$.(A visualization is shown in Fig (2.4))

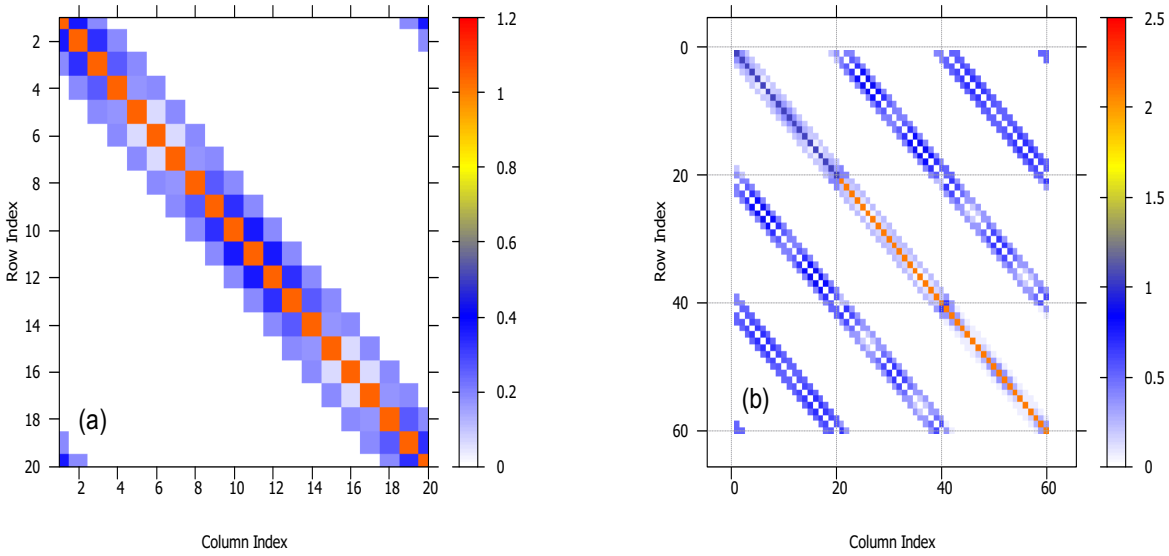

Hình 2.6: An easy and intuitive visualization of sub-matrix h_0 one band(left) and matrix H all band(right) through standard plotter with $q = 20$. Left: orange squares, dark blue squares and sky blue squares are equivalent to $\epsilon_1, 2t_0 \cos\zeta_1, t_0$ respectively.

An alternative approach to the derivation of the Hamiltonian under an uniform magnetic field is given in Appendix B.

2.3 Spin-orbit coupling

Due to the heavy mass of the transistion-metal M atom, its spin orbit coupling(SOC) can be large. For the sake of simplicity, only the on-site contribution, namely, the $\mathbf{L}\cdot\mathbf{S}$ term from M atoms. Using the bases $\left\{\left|d_{z^2},\uparrow\right\rangle, \left|d_{xy},\uparrow\right\rangle, \left|d_{x^2-y^2},\uparrow\right\rangle, \left|d_{z^2},\downarrow\right\rangle, \left|d_{xy},\downarrow\right\rangle, \left|d_{x^2-y^2},\downarrow\right\rangle\right\}$, we get the SOC contribution to the Hamiltonian as

$$H^{'} = \lambda\mathbf{L}\cdot\mathbf{S} = \frac{\lambda}{2}\begin{pmatrix} L_z & L_x - iL_y \\ L_x + iL_y & -L_z \end{pmatrix}, \tag{2.28}$$

in which

$$L_z = \begin{pmatrix} 0 & 0 & 0 \\ 0 & 0 & 2i \\ 0 & -2i & 0 \end{pmatrix} \tag{2.29}$$

is the matrix of $\hat{L}_z$(z component of the orbital angular momentum) in bases of $d_{z^2}, d_{xy}, d_{x^2-y^2}$ and λ is characterized the strength of the SOC. Noting that, under the three bases, the matrix elements of $\hat{L}_x$ and $\hat{L}_y$ are all zeros. There for the Hamiltonian for the magnetic

unit cell with the SOC as follows

$$\begin{aligned} H_{\mathrm{SOC}}(\mathbf{k}) &= \mathbf{I}_2 \otimes H_0(\mathbf{k}) + H^{'} \\ &= \begin{pmatrix} H_{3q\times 3q}(\mathbf{k}) + \frac{\lambda}{2}L_z & 0 \\ 0 & H_{3q\times 3q}(\mathbf{k}) - \frac{\lambda}{2}L_z \end{pmatrix} \end{aligned} \tag{2.30}$$

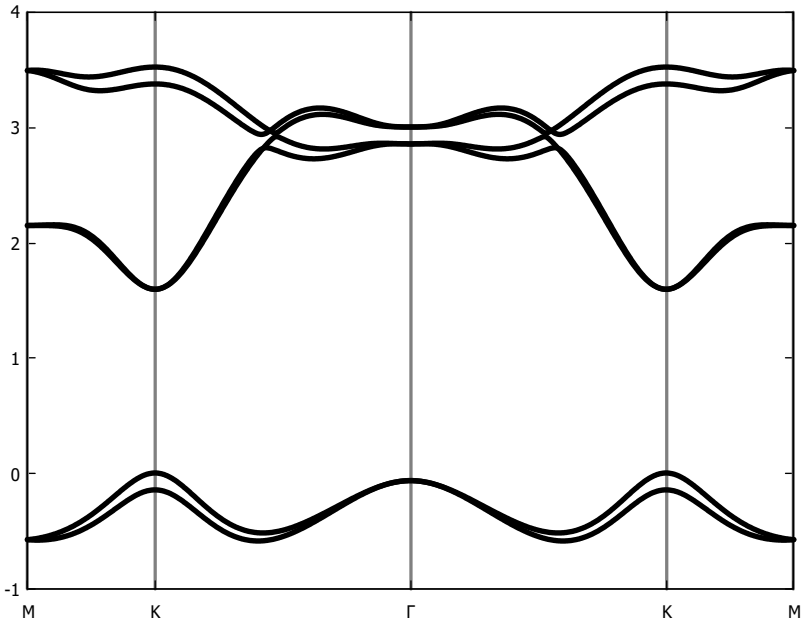

Hình 2.7

2.4 Landau levels

In solid-state physics, the behavior of electrons in magnetic fields is usually introduced by using the Hamiltonian

$$H = \frac{\mathbf{p} + e\mathbf{A}(\mathbf{r})^2}{2m}, \tag{2.31}$$

and the energy eigenfunctions are known as Landau levels

$$E = \left(n + 1/2\right)\hbar\omega_c. \tag{2.32}$$

This treatment is for free electrons,[4] but near the bottom of the two-dimensional tight-binding band of TMD, the energy is approximately free-electron-like by Taylor

expasion to second order of $\mathbf{k}$

$$\begin{aligned} H(\mathbf{k}) &\approx 2t_0 \left[1 - \frac{a^2k_x^2}{2} + 2\left(1 - \frac{a^2k_x^2}{8}\right)\left(1 - \frac{3a^2k_y^2}{8}\right)\right] \\ &= t_0\frac{3}{16}\left(32 + a^4k_x^2k_y^2\right) - t_0\frac{3}{2}a^2\left(k_x^2 + k_y^2\right) + \epsilon_1, \end{aligned} \tag{2.33}$$

the first term a^2 is negligibly small and another can be treated like constant, then we have

$$H(\mathbf{k}) \approx 6t_0 - \frac{3}{2}t_0a^2(k_x^2 + k_y^2) + \epsilon_1. \tag{2.34}$$

One of the ways derivation of effective mass m^* is substitution $\mathbf{k} \to \mathbf{p}+e\mathbf{A}$, with Landau gauge $\mathbf{A} = (0, Bx, 0)$

$$\begin{aligned} H(\mathbf{p}) &\approx 6t_0 - \frac{3}{2}t_0\frac{a^2}{\hbar^2}\left[p_x^2 + \left(p_y + eBx\right)^2\right] + \epsilon_1 \\ &\approx 6t_0 - \frac{3}{2}t_0\frac{a^2}{\hbar^2}p_x^2 - \frac{3}{2}t_0\frac{a^2}{\hbar^2}(eB)^2\left[x - \left(-\frac{\hbar k_y}{eB}\right)\right]^2 + \epsilon_1. \end{aligned} \tag{2.35}$$

The Eq (2.24) can be rewrite in the form as

$$E(\mathbf{p}) = 6t_0 - \left[\frac{1}{2m^*}p_x^2 + \frac{1}{2}m^*\omega_c^2(x - x_0)^2\right] + \epsilon_1, \tag{2.36}$$

where $m^* = \dfrac{\hbar^2}{(3t_0a^2)}$ is the effective mass and $x_0 = \frac{\hbar k_y}{eB}$. Hence, the cyclotron frequency is

$$\omega_c = \frac{eB}{m^*} = \frac{8\pi\sqrt{3}t_0}{\hbar}\frac{p}{q}, \tag{2.37}$$

and therefore the Landau levels near the bottom of the band $|d_{z^2}\rangle$ can be written as

$$\begin{aligned} E &= 6t_0 - \hbar\omega_c(n + 1/2) + \epsilon_1 \\ &= t_0\left(6 - 8\pi\sqrt{3}\frac{p}{q}(n + 1/2)\right) + \epsilon_1, \end{aligned} \tag{2.38}$$

in linear order of an uniform-flux, where n is Landau index.

In Fig 2.7 we compare the spectrum of a small section of triangular lattice with $p/q = 1/797$, which is equivalent to small magnetic field, the spectrum of MoS_2, with the energy of Landau levels given by Eq.(2.38) show standard equally spaced Landau levels[5,6,7,8] near the bottom of the bands, as plotted in Fig 2.7(b). The fan of Landau

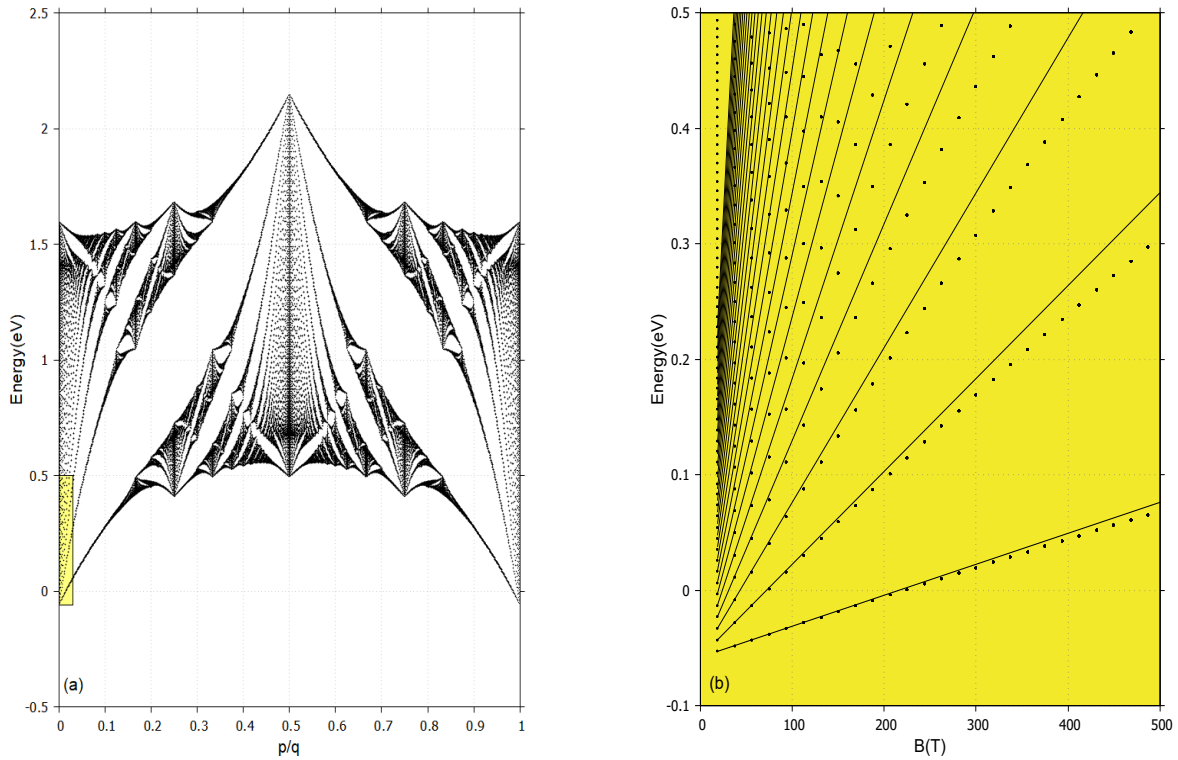

Hình 2.8: (a) Same plot as Fig 2.3 but we consider a small area and (b) is the Landau fan diagram show for the first $n = 30$ levels near the bottom of the conduction band for a magnetic field up to $B = 500\ T$.

levels can be clearly seen emergin from the partern in Fig 2.4(a). The Landau levels are all close to being linear in B, resulting from the magnetic quantization of parabolic bands at $B = 0$. In our model study, Landau levels can be classified into specific groups. In each group, each levels can be further labeled by a Landau index n. Figure 2.4 displays a blowup of the low uniform magnetic region and the LLs as a function of $\Phi/{\Phi_0}^9$.

In Fig 2.7, there is just one band in case zero field, with the effective mass $m^* = \frac{\hbar}{3t_0a^2}$. The numerical result for this portion of the spectrum are shown in Fig 2.7 for $p/q \geq 1/797$. The first few Landau levels are clearly seen, and the asymtotic slopes p/q at large q given by Eq. (2.38) are shown for comparison for the first five Landau levels at $B \leq 100$T. At the values of B the fit is not ideal, but it does seem to be improving with the decreasing f.

More interesting is the top and bottom of conduction and valence band of the zero field spectrum. In order to determine the cyclotron frequency for the three-band, through the derivation in Appendix C, we have obtained the Landau levels for the three-band model when the field is turned on

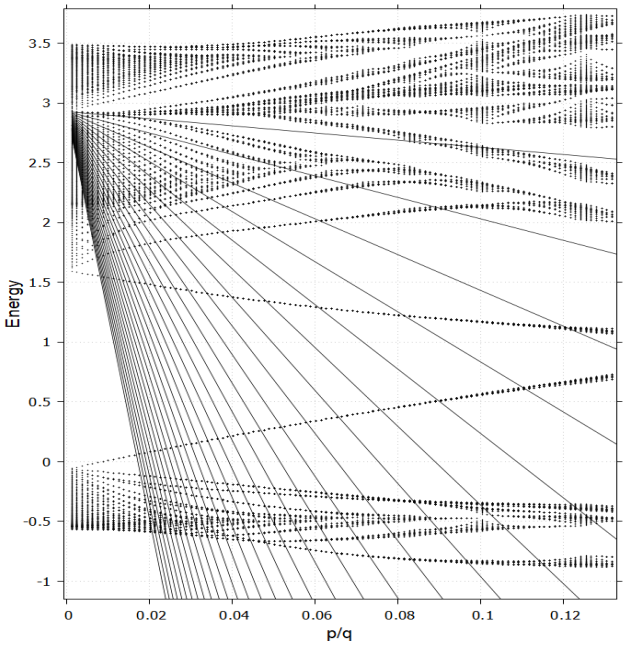

Hình 2.9

Ta có thể thấy một số mức Landau có năng lượng là được tăng tuyến tính với cường độ từ trường, nhưng nó lại không cách đều và chính xác như hình của Hofstadter butterfly. Trong trường hợp một band, khối lượng hiệu dụng m^* và điện tích là đủ để mô tả được phổ Landau theo sự thay đổi tuyến tính của từ trường. Trong trường hợp 2 band và 3 band thì

CHƯƠNG 3

DISCUSSION AND FUTURE WORK

REFERENCES

[1] Gui-Bin Liu, Wen-Yu Shan, Yugui Yao, Wang Yao, and Di Xiao. Three-band tight-binding model for monolayers of group-vib transition metal dichalcogenides. *Phys. Rev. B*, 88:085433, Aug 2013.

[2] Fırat Yalçın. Tight binding investigation of graphene nanostructures under magnetic field. Master's thesis, Middle East Technical University, 2019.

[3] Douglas R. Hofstadter. Energy levels and wave functions of bloch electrons in rational and irrational magnetic fields. *Phys. Rev. B*, 14:2239–2249, Sep 1976.

[4] James G. Analytis, Stephen J. Blundell, and Arzhang Ardavan. Landau levels, molecular orbitals, and the hofstadter butterfly in finite systems. *American Journal of Physics*, 72(5):613–618, 05 2004.

[5] D. Shoenberg. *Magnetic Oscillations in Metals*. Cambridge Monographs on Physics. Cambridge University Press, 1984.

[6] J. Singleton. *Band Theory and Electronic Properties of Solids*. Oxford Master Series in Condensed Matter Physics. OUP Oxford, 2001.

[7] S. Blundell. *Magnetism in Condensed Matter*. Oxford Master Series in Condensed Matter Physics 4. OUP Oxford, 2001.

[8] C. Kittel. *Quantum Theory of Solids*. Wiley, 1987.

[9] Juan Li, Yi-Fei Wang, and Chang-De Gong. Tight-binding electrons on triangular and kagomé lattices under staggered modulated magnetic fields: quantum hall effects and hofstadter butterflies. *Journal of Physics: Condensed Matter*, 23(15):156002, apr 2011.

[10] Andor Kormányos, Viktor Zólyomi, Neil D. Drummond, Péter Rakyta, Guido Burkard, and Vladimir I. Fal'ko. Monolayer mos_2: Trigonal warping, the Γ valley, and spin-orbit coupling effects. *Phys. Rev. B*, 88:045416, Jul 2013.

[11] Fengyuan Xuan and Su Ying Quek. Valley zeeman effect and landau levels in two-dimensional transition metal dichalcogenides. *Phys. Rev. Res.*, 2:033256, Aug 2020.

[12] Jun John Sakurai and Jim Napolitano. *Modern quantum mechanics*. Cambridge University Press, 2020.

[13] Philip George Harper. The general motion of conduction electrons in a uniform magnetic field, with application to the diamagnetism of metals. *Proceedings of the Physical Society. Section A*, 68(10):879–892, 1955.

[14] Yakir Aharonov and David Bohm. Significance of electromagnetic potentials in the quantum theory. *Physical review*, 115(3):485–497, 1959.

[15] Rudolph Peierls. Zur theorie des diamagnetismus von leitungselektronen. *Zeitschrift für Physik*, 80(11):763–791, 1933.

[16] Gi-Yeong Oh. Energy spectrum of a triangular lattice in a uniform magnetic field: Effect of next-nearest-neighbor hopping. *Journal of the Korean Physical Society*, 37(5):534–539, 2000.

[17] Jenö Sólyom. *Fundamentals of the Physics of Solids: Volume II: Electronic Properties*, volume 2. Springer Science & Business Media, 2008.

[18] David J Griffiths and Darrell F Schroeter. *Introduction to quantum mechanics*. Cambridge university press, 2018.

APPENDIX A

Construct matrix

In Ref.[1],G-B Liu *et al*. contructed

APPENDIX B

Harper's equation

Ta xét phương trình Harper cho trường hợp mạng tinh thể là mạng vuông được cho bởi Hamiltonian từ ví dụ trong bài[2]

$$\begin{aligned} H(\mathbf{k}) &= 2t\left[\cos(k_x a) + \cos\big(k_y a\big)\right] \\ &= t\left[e^{ik_x a} + e^{-ik_x a} + e^{ik_y a} + e^{-ik_y a}\right] \end{aligned} \tag{B.1}$$

Bằng cách áp dụng Peierls's substitution $\mathbf{k} \to (\vec{p} - e\mathbf{A})/\hbar$, ta có

$$\begin{aligned} H &= t\left[e^{ik_x a} + e^{-ik_x a} + e^{i(p_y - eBx)a/\hbar} + e^{-i(p_y - eBx)a/\hbar}\right] \\ &= t\left[e^{ik_x a} + e^{-ik_x a} + e^{ip_y a/\hbar}e^{i2\pi Bx/\Phi_0} + e^{-ip_y a/\hbar}e^{-i2\pi Bx/\Phi_0}\right] \end{aligned} \tag{B.2}$$

Thay $x = ma$ và $y = na$ cho toạ độ của mạng tinh thể vuông, ta thu được phương trình Harper

Let us consider the case of hexagonal lattice with $|d_{z^2}\rangle$ band as a basis under an uniform magneticc field given by the Landau gauge $\vec{A} = (0, Bx, 0)$. Given

$$
\begin{aligned}
h_0 &= 2t_0\left(\cos 2\alpha + 2\cos\alpha\cos\beta\right) + \epsilon_1 \\
&= 2t_0\left[\cos(k_x a) + 2\cos\left(\frac{k_x a}{2}\right)\cos\left(\frac{\sqrt{3}k_y a}{2}\right)\right] + \epsilon_1 \\
&= 2t_0\left\{\cos(k_x a) + \cos\left[\left(k_x + \sqrt{3}k_y\right)\frac{a}{2}\right] + \cos\left[\left(k_x - \sqrt{3}k_y\right)\frac{a}{2}\right]\right\} + \epsilon_1 \\
&= 2t_0\left\{\cos\left(p_x\frac{a}{\hbar}\right) + \cos\left[\left(p_x + \sqrt{3}eBx + \sqrt{3}p_y\right)\frac{a}{2\hbar}\right]\right. \\
&\left. + \cos\left[\left(p_x - \sqrt{3}eBx - \sqrt{3}p_y\right)\frac{a}{2\hbar}\right]\right\} + \epsilon_1 \\
&= t_0\Big[e^{ip_x\frac{a}{\hbar}} + e^{-ip_x\frac{a}{\hbar}} + e^{i(p_x+\sqrt{3}eBx+\sqrt{3}p_y)a/2\hbar} + e^{-i(p_x+\sqrt{3}eBx+\sqrt{3}p_y)a/2\hbar} \\
&+ e^{i(p_x-\sqrt{3}eBx-\sqrt{3}p_y)a/2\hbar} + e^{-i(p_x-\sqrt{3}eBx-\sqrt{3}p_y)a/2\hbar}\Big] + \epsilon_1.
\end{aligned}
\tag{B.3}
$$

We replaced $\hbar k$ in the above function by the operators $\vec{p} - e\vec{A}/c$ in order to create an operator out of h_0. When this substitution is made, the Hamiltonian element is seen to contain translation operators $\exp\left[ap_x/\hbar\right], \exp\left[a\sqrt{3}p_y/(2\hbar)\right]$. Depending on the gauge chosen, there are, in addition, certain phase factors dependent on the magnetic field strength, which multiply the translation operators. The Landau gauge was $\vec{A} = (0, Bx, 0)$ was chosen, then only the translation along y are multiplied by phases.[3] Applying the BCH's formula and taking to account the commutation relation $[x, p_x] = i\hbar$

$$
\begin{aligned}
e^{\pm i(p_x+\sqrt{3}eBx)a/2\hbar} &= e^{\pm ip_x a/2\hbar}e^{\pm i\sqrt{3}eBxa/2\hbar}e^{-\frac{1}{2}\left[\pm ip_x, \pm i\sqrt{3}eBx\right]a^2/2\hbar^2} \\
&= e^{\pm ip_x a/2\hbar}e^{\pm i\sqrt{3}eBxa/2\hbar}e^{\mp i\sqrt{3}eBa^2/8\hbar}
\end{aligned}
\tag{B.4}
$$

Substituting $x = \dfrac{ma}{2}$ into (B.2), this leads to

$$
e^{\pm i(p_x+\sqrt{3}eBx)a/2\hbar} = e^{\pm ip_x a/2\hbar}e^{\pm i\sqrt{3}eB(m+1/2)a^2/4\hbar} \tag{B.5}
$$

And

$$
\begin{aligned}
e^{\pm i(p_x-\sqrt{3}eBx)a/2\hbar} &= e^{\pm ip_x a/2\hbar}e^{\mp i\sqrt{3}eBxa/2\hbar}e^{-\frac{1}{2}\left[\pm ip_x, \mp i\sqrt{3}eBx\right]a^2/2\hbar^2} \\
&= e^{\pm ip_x a/2\hbar}e^{\mp i\sqrt{3}eBxa/2\hbar}e^{\mp i\sqrt{3}eBa^2/8\hbar}
\end{aligned}
\tag{B.6}
$$

Substituting $x = \dfrac{ma}{2}$ into (B.4), this leads to

$$
e^{\pm i(p_x-\sqrt{3}eBx)a/2\hbar} = e^{\pm ip_x a/2\hbar}e^{\mp i\sqrt{3}eB(m-1/2)a^2/4\hbar} \tag{B.7}
$$

The operators $e^{\pm ip_x a/2\hbar}, e^{\pm ip_y\sqrt{3}a/2\hbar}$ can be regconized as translational operators, we can rewrite (B.3) as

$$\begin{aligned} &t_0\varphi_1(x+a,y)+t_0\varphi_1(x-a,y)+t_0\varphi_1(x+\frac{a}{2},y+\frac{a\sqrt{3}}{2})e^{\frac{ie}{\hbar}B(m+1/2)\frac{a^2\sqrt{3}}{4}} \\ &+t_0\varphi_1(x+\frac{a}{2},y-\frac{a\sqrt{3}}{2})e^{-\frac{ie}{\hbar}B(m+1/2)\frac{a^2\sqrt{3}}{4}}+t_0\varphi_1(x-\frac{a}{2},y+\frac{a\sqrt{3}}{2})e^{\frac{ie}{\hbar}B(m+1/2)\frac{a^2\sqrt{3}}{4}} \\ &+t_0\varphi_1(x-\frac{a}{2},y-\frac{a\sqrt{3}}{2})e^{-\frac{ie}{\hbar}B(m-1/2)\frac{a^2\sqrt{3}}{4}}+\epsilon_1\varphi_1(x,y)=E_1\varphi_0(x,y), \end{aligned} \tag{B.8}$$

for the sake of simplicity let us define $\varphi_0 \equiv |d_{z^2}\rangle$.
It is reasonable to assume planewave behavior in the y direction, since the coefficents in the above equation only involve x. Therefore, we can assume the partial solution for y to be in the form

$$\varphi(\frac{ma}{2},\frac{na\sqrt{3}}{2})=e^{ik_y n\frac{a\sqrt{3}}{2}}G(m), \tag{B.9}$$

which reduces (B.6) to

$$\begin{aligned} &t_0\varphi_0(m+2)+t_0\varphi_0(m-2)+t_0\varphi_0(m+1)e^{2i\pi(m+1/2)p/q}e^{ik_y a\sqrt{3}/2} \\ &+t_0\varphi_0(m+1)e^{-2i\pi(m+1/2)p/q}e^{-ik_y a\sqrt{3}/2}+t_0\varphi_0(m-1)e^{2i\pi(m-1/2)p/q}e^{ik_y a\sqrt{3}/2} \\ &+t_0\varphi_0(m-1)e^{-2i\pi(m-1/2)p/q}e^{-ik_y a\sqrt{3}/2}+\epsilon_1\varphi_0(m)=E_1\varphi_0(m), \end{aligned} \tag{B.10}$$

this is equivalent to Eq. 2.16 we have mentioned in Section 2.2. Equation B.7 is sometimes called "Harper's equation".[13] Since different m values give different equations, one reaches a unique set of equations when Φ/Φ_0 is a rational number p/q and m goes through q different values, essentially resulting in the Hamiltonian matrix written for a magnetic unit cell enlarged in x direction q times.
Trong trường hợp của TMD của[1] đã đưa ra thì ta đã bỏ qua đi đóng góp của nguyên tử X, dẫn đến cấu trúc mạng tinh thể của TMD lục giác trở thành mạng tam giác bình thường và từ đó ta có thể mapping từ mạng tam giác thành trường hợp của mạng vuông. Ở mạng tam giác ta đã đưa ra được rằng các toán tử tịnh tiến phải tuân theo công thức Baker-Campbell-Hausdorff.

APPENDIX C

Cyclotron frequency for all band

Hamiltonian in the new basis read

$$\begin{aligned}\tilde{H}^{NN}(\mathbf{k}) &= WH^{NN}(\mathbf{k})W^{\dagger} \\ &= \begin{pmatrix} \frac{1}{2}(h_{11}+h_{22}+2\,\mathrm{Im}[h_{12}]) & \frac{1}{\sqrt{2}}(h_1^*+ih_2^*) & \frac{1}{2}(h_{11}-h_{22}+2i\,\mathrm{Re}[h_{12}]) \\ \frac{1}{\sqrt{2}}(h_1-ih_2) & h_0 & \frac{1}{\sqrt{2}}(h_1+ih_2) \\ \frac{1}{2}(h_{11}-h_{22}-2i\,\mathrm{Re}[h_{12}]) & \frac{1}{\sqrt{2}}(h_1^*-ih_2^*) & \frac{1}{2}(h_{11}+h_{22}-2i\,\mathrm{Im}[h_{12}]) \end{pmatrix}\end{aligned} \tag{C.1}$$

Hamiltonian matrix element for the valence band now is

$$\begin{aligned} h_v =& \frac{1}{2}\left(h_{11}+h_{22}+2\,\mathrm{Im}[h_{12}]\right) \\ =& (t_{11}+t_{22})\cos 2\alpha + 2\,(t_{11}+t_{22})\cos\alpha\cos\beta \\ &+ 4t_{12}\sin\alpha(\cos\alpha-\cos\beta)+\epsilon_2 \\ =& (t_{11}+t_{22})\cos k_x a + 2\,(t_{11}+t_{22})\cos\frac{k_x a}{2}\cos\frac{\sqrt{3}k_y a}{2} \\ &+ 4t_{12}\sin\frac{k_x a}{2}(\cos\frac{k_x a}{2}-\cos\frac{\sqrt{3}k_y a}{2})+\epsilon_2. \end{aligned} \tag{C.2}$$

By using Taylor's expansion to second order of $\mathbf{k}$ on (C.2) we have

$$\begin{aligned} h_v \approx& (t_{11}+t_{22})\left(1-\frac{a^2k_x^2}{2}\right)+2(t_{11}+t_{22})\left(1-\frac{a^2k_x^2}{8}\right)\left(1-\frac{3a^2k_y^2}{8}\right) \\ &- 4t_{12}\frac{ak_x}{2}\left(\frac{a^2k_x^2}{8}-\frac{3a^2k_y^2}{8}\right)+\epsilon_2 \\ \approx& 3(t_{11}+t_{22})-\frac{3a^2(t_{11}+t_{22})}{4}\left(k_x^2+k_y^2\right)-\frac{a^3t_{12}\left(k_x^2-3k_y^2\right)}{4} \\ &+\frac{6a^4(t_{11}+t_{22})}{32}k_x^2k_y^2+\epsilon_2. \end{aligned} \tag{C.3}$$

In this (C.3), we neglect coefficents of terms a^3 and a^4, this leads to

$$h_v \approx 3(t_{11}+t_{22}) - \frac{3a^2(t_{11}+t_{22})}{4}\left(k_x^2+k_y^2\right)\epsilon_2, \tag{C.4}$$

and using substitution $\hbar\mathbf{k} \to (\mathbf{\Pi}+e\mathbf{A})/\hbar$

$$h_v \approx 3(t_{11}+t_{22}) - \frac{3a^2(t_{11}+t_{22})}{4\hbar^2}\left[\Pi_x^2+(\Pi_y+eBx)^2\right] + \epsilon_2, \tag{C.5}$$

Instead of doing as we have done in Section 2, there is an alternative way to determine the energy spectrum. The Hamiltonian can be simplified by a suitably chosen canonical transformation, or ladder (creation and annihilation) operators can be used instead of position and momentum operators, but the description of the motion in the xy-plane requires two commuting sets of operators now. Since x and Π_y appear together in the combination $x+\frac{1}{eB}\Pi_x$, the appropriate choice in this case is[17,18]

$$\begin{aligned}
a &= \sqrt{\frac{eB}{2\hbar}}\left(x+\frac{1}{eB}\Pi_y+\frac{i}{eB}\Pi_x\right),\\
a^\dagger &= \sqrt{\frac{eB}{2\hbar}}\left(x+\frac{1}{eB}\Pi_y-\frac{i}{eB}\Pi_x\right),\\
b &= \sqrt{\frac{eB}{2\hbar}}\left(y+\frac{1}{eB}\Pi_x+\frac{i}{eB}\Pi_y\right),\\
b^\dagger &= \sqrt{\frac{eB}{2\hbar}}\left(y+\frac{1}{eB}\Pi_x-\frac{i}{eB}\Pi_y\right).
\end{aligned} \tag{C.6}$$

The inverse transformation is then

$$\begin{aligned}
x+\frac{1}{eB}\Pi_y &= \sqrt{\frac{\hbar}{2eB}}\left(a+a^\dagger\right),\\
\Pi_x &= i\sqrt{\frac{\hbar eB}{2}}\left(a^\dagger-a\right),\\
y+\frac{1}{eB}\Pi_y &= \sqrt{\frac{\hbar}{2eB}}\left(b+b^\dagger\right),\\
\Pi_y &= i\sqrt{\frac{\hbar eB}{2}}\left(b^\dagger-b\right).
\end{aligned} \tag{C.7}$$

It follows from the cannonical commutation relations of the position and momentum operators that the ladder operators satisfy bosonic commutation relations

$$[a,a^\dagger]=1, \quad [b,b^\dagger]=1, \tag{C.8}$$

and

$$[a, a] = [a^\dagger, a^\dagger] = [b, b] = [b^\dagger, b^\dagger] = 0, \tag{C.9}$$

moreover the operators $a(a^\dagger)$ and $b(b^\dagger)$ commute with each other, too. In terms of them, the Hamiltonian (C.5) can be cast in form

$$content... \tag{C.10}$$

The cyclotron frequency is

$$w_c = \frac{eB}{m^*} = \frac{4\pi\sqrt{3}(t_{11} + t_{22})}{\hbar}\frac{p}{q}, \tag{C.11}$$

and

$$E \approx (t_{11} + t_{22})\left(3 - 4\pi\sqrt{3}\frac{p}{q}(n + 1/2)\right) + \epsilon_2, \tag{C.12}$$

is the Landau levels near the top of the valence band.